EAI SESC 2022 – 4th EAI International Conference on Sustainable Energy for Smart Cities

Modular Multilevel Converter: A Comparison of Pulse-Width Modulation and Current Control Techniques

Nuno Rodrigues[1], Jose Cunha[1], José Afonso[1], Vitor Monteiro[1] and Joao L. Afonso[1]

[1] ALGORITMI Research Center / LASI, University of Minho, Guimaraes, Portugal

Abstract. With the constant increase of power converters in industry, the study and comparison of control techniques for these converters are of paramount importance to optimize their functioning, as well as to improve their efficiency. This paper presents a comparison of the most relevant digital control techniques of pulse-width modulation and current control for a modular multilevel converter (MMC), which is a power converter that is increasing in popularity among researchers, and with a steady growth in its literature. Beginning with a theoretical presentation of each control technique and using explanatory figures and computational results, the focus of this paper is the understanding of the modulation and control techniques for the MMC. Since the MMC has a modular structure, the power is distributed among the different submodules, which increases the complexity of the control system. Furthermore, a balancing strategy for the voltage across the capacitor of each submodule of the MMC is also presented. Along with the paper, computer simulations are presented, which were carried out to validate the functioning of the MMC and the control techniques, as well as to understand the differences in the obtained results.

Keywords: Power Electronics, Modular Multilevel Converter, Digital Control.

1 Introduction

Nowadays, the number of applications that requires power electronics converters is continuously increasing with a specific preponderance for electric vehicles, renewables, storage systems, power conditioners, and power grid systems [1]. In terms of power converters, several topologies can be considered, including traditional topologies, multilevel topologies, and interleaved topologies, both in terms of voltage-source or current-source [2]. Since the importance of multilevel topologies for a wide range of applications, this paper deals with the analysis of the modular multilevel converter (MMC). When connected to the power grid, the MMC requires dedicated control algorithms, including current control in the power grid interface, voltage control of the DC-link capacitors, and the modulation, aiming to optimize the performance of the converter, and mitigate power quality problems [3]. Along the last decades, relevant digital control strategies were proposed with different levels of complexity [4]. In this context,

this paper presents a comparison of pulse-width modulation and current control techniques for the MMC.

The rest of this article is organized as: section 2 presents a comparison between phase shift carrier PWM and level-shift carrier PWM; section 3 presents a comparison between current control techniques, namely the PI and model predictive, as well as the control strategy for the capacitor voltage balancing; section 4 presents a computation validation of the power converter and discussed techniques; and section 5 finalizes the paper with the conclusions.

2 Modulation Techniques for MMC

When it comes to PWM techniques for power electronics converters with 2 or 3 voltage levels, the options available in the literature are extensive. However, regarding in specific the PWM techniques for MMC, and since it requires different stages for each submodule, it results in more complex techniques for synthesizing the desired multilevel waveform [5]. The modulation consists of a comparison between a modulator waveform, which takes the form of the desired signal, and one or more triangular carrier waveforms, where their disposition varies depending on the technique. In this section, it is presented a comparison between the most conventional, namely the phase-shift carrier PWM and the level-shift carrier PWM [6].

2.1 Phase-Shift Carrier PWM

In phase-shit carrier PWM, all the triangular carrier signals have the same: frequency; peak-to-peak amplitude; and offset value. However, varies the phase disposition of the triangular carriers. The carrier signals are disposed with a $2\pi/N$ phase-shift between them, where N represents the number of submodules in each arm of the MMC.

Fig. 1 illustrates the referred modulation technique for a MMC with two submodules in each arm, therefore with $N = 2$. For a better understanding of the technique through visualization of the waveforms of the carrier signals and the modulator signals, the modulator signals were disposed with 50 Hz frequency and the carrier signals with 500 Hz frequency. In a practical implementation, typically, this frequency would be higher, in the order of kHz to a few tens of kHz. In this figure, V_{ref_up} corresponds to the reference of the up arm, V_{ref_down} to the corresponds to the reference of the down arm, while V_{tri1} and V_{tri2} corresponds to the reference of the necessary two carriers with a phase disposition of 180 degrees. The variables V_{pwm1_up}, V_{pwm2_up}, V_{pwm1_down}, V_{pwm1_down}, as well as the corresponding complementary values, corresponds to the gate pulse-pattern of the switches that constitute the MMC with 2 submodules.

The phase-shift technique is very interesting for MMC due to some unique characteristics, such as: even power losses across the submodules of the converter; minimizes DC-link voltage ripple; and provides a natural balancing of submodule capacitors voltage at the carrier frequency [7]. Although being very advantageous for multilevel topologies, this technique does not possess sensibility to DC-link voltage fluctuations [8].

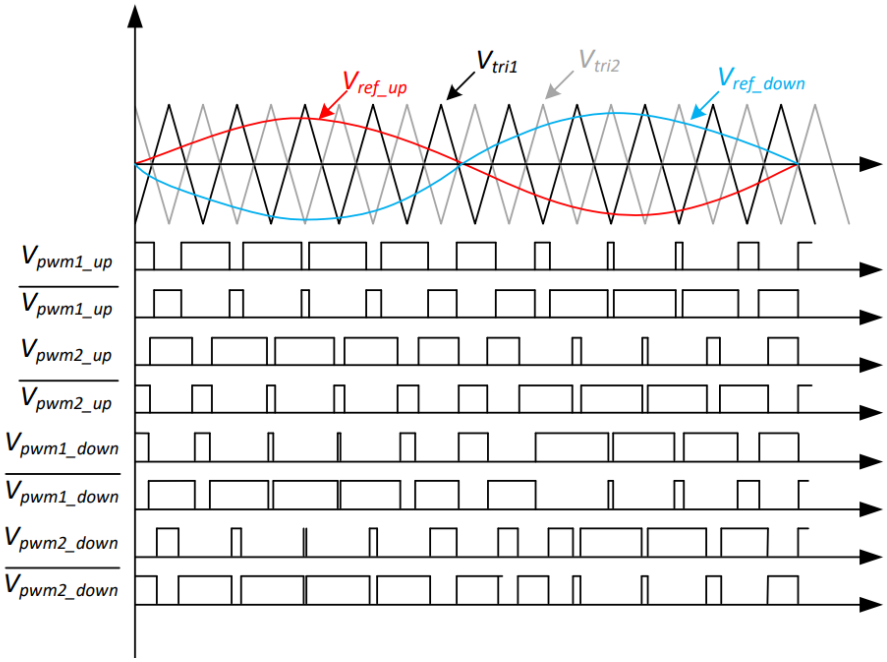

Fig. 1. Phase-shift carrier modulation technique for a MMC with 2 submodules in each arm.

2.2 Level-Shift Carrier PWM

In level-shift PWM, the required number of triangular carriers is the same when compared with the phase-shift, with all the triangular carrier signals sharing the same frequency and peak-to-peak amplitude, however, varying in the offset value since they are vertically disposed. There are many variants of this technique, where the phase disposition of the triangular carries varies.

Similar to the figure presented to the phase shift carrier technique, **Fig. 2** presents the level-shift modulation for a MMC with 2 submodules in each arm. Also in this technique, with the objective of facilitating the understanding, 50 Hz modulator signals and 500 Hz carrier signals were considered.

This technique is very popular in conventional multilevel converters, not being very advantageous however for the MMC, since it causes uneven power losses across the submodules, resulting in voltage ripple in the submodule capacitors and high circulating currents [9].

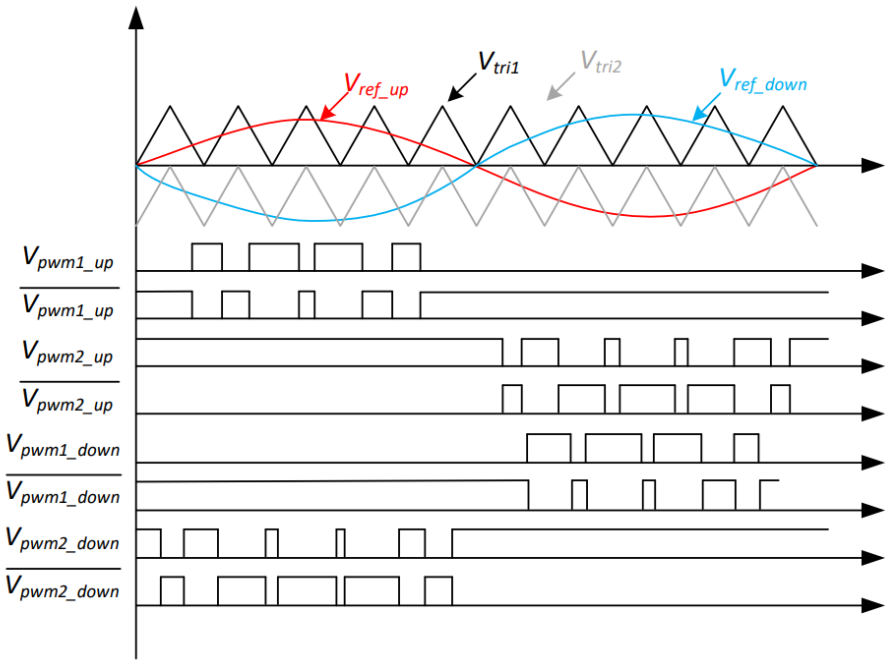

Fig. 2. Level-shift modulation technique for a MMC with 2 submodules in each arm.

3 Current Control Techniques

Regarding the control of power electronics converters, digital control schemes allow an efficient, safe, and reliable operation, with higher dynamic and steady-state performance. In **Fig. 3** is presented a block diagram where the different steps for controlling the MMC are shown.

This section focus lies on the control of the output current, as well as the balancing of the capacitor voltage across every submodule since the functioning of the power converter depends on these two controls. Regarding the circulating currents, it is considered a secondary control since the function of the converter does not depend on it. However, it is also important because the circuiting currents lead to higher RMS values on the arm currents, resulting in power losses and decrease of efficiency.

3.1 PI Current Controller

The PI controller aims to control the MMC current according to a current reference. In a first stage, it is calculated the error between the reference current and the output current of the MMC and then, such error serves as input for the PI controller, which consists of a proportional and integral gains, and an integral parcel, presented in the following equation [10]:

$$V_{mod} = K_p(i_{ref} - i_{out}) + K_i \int_0^t (i_{ref} - i_{out})dt \quad (1)$$

This technique requires the tuning of the proportional and integral gains for a better performance of the system, keeping in mind that the dynamic response is limited by the PI gains as well as the steady state error, which can be mitigated, but never fully extinguished[11].

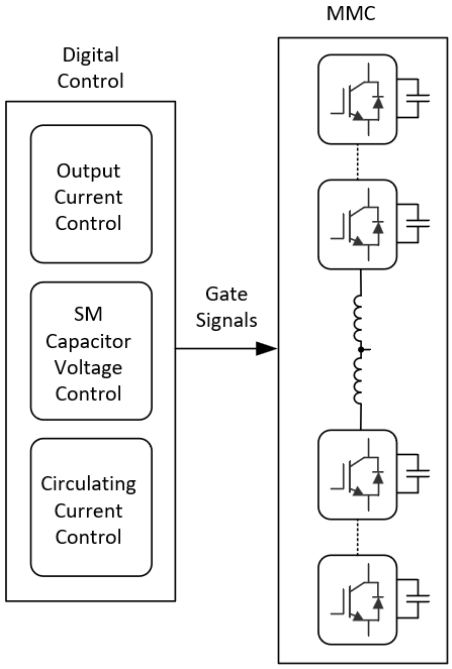

Fig. 3. Block diagram of the MMC control system.

The output of the PI controller corresponds to the input of the modulation block, v_{mod}, whose output results in the command signals for the switching power devices, as presented in **Fig. 4**. As the command signals, v_{com}, are generated by a modulation technique, the switching frequency of the semiconductors has a fix value, making it easier for the dimensioning of the passive filters of the converter.

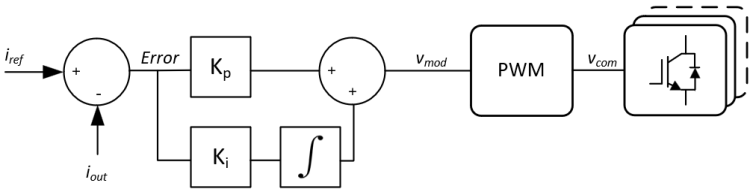

Fig. 4. PI controller with PWM.

3.2 Model Predictive Current Control

The model predictive control calculates the desired control variables based on an electrical model of the converter in study, without any integral error associated as appear in the PI controller [3]. This type of controller, typically, presents fast transient response, and small-steady state error, due to its fast dynamic response [12].

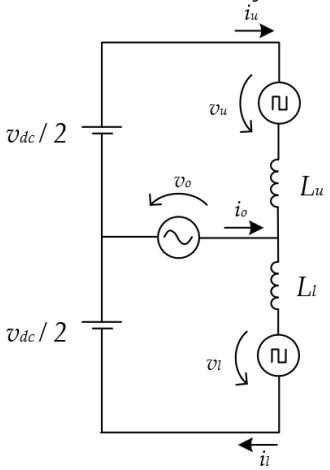

Fig. 5. MMC equivalent circuit.

In order to be able to obtain the electrical model of the MMC, its equivalent circuit is presented in **Fig. 5**. The circulating current will be neglected for a simplification of the model. Applying Kirchhoff's voltage law on the equivalent circuit, and disregarding the conduction and switching losses on the semiconductors, the equations obtained are the following:

$$v_o = -L_u \frac{di_u}{dt} - v_u - i_u R_{Lu} \tag{2}$$

$$v_o = L_l \frac{di_l}{dt} + v_l + i_l R_{Ll} \tag{3}$$

The predictive control is a current based controller, in which the control variable in each equation is the current flowing in the arm.

$$i_{u_{error}} = i_{u_{ref}} - i_u \tag{4}$$

$$i_{l_{error}} = i_{l_{ref}} - i_l \tag{5}$$

The voltage drop in the internal resistance of the inductive filters of the arms of the MMC can be neglected ($i_l R_{Ll}$ and $i_u R_{Lu}$), due to the low value that they have, thus resulting in a simplification of the equations without any significant error associated.

$$v_o = -L_u \frac{d\left(i_{u_{ref}} - i_{u_{error}}\right)}{dt} - v_u \tag{6}$$

$$v_o = L_l \frac{d\left(i_{l_{ref}} - i_{l_{error}}\right)}{dt} + v_l \tag{7}$$

Separating the differential part in the previous equations:

$$v_o = -L_u \frac{di_{u_{ref}}}{dt} + L_u \frac{i_{u_{error}}}{dt} - v_u \tag{8}$$

$$v_o = L_l \frac{di_{l_{ref}}}{dt} - L_l \frac{i_{l_{error}}}{dt} + v_l \tag{9}$$

Since the control is performed by a microcontroller, the equations need to be in discrete time, instead of linear time. The discretization of the derivative can be done using Euler's method:

$$\frac{dx}{dt} \cong \frac{x(k) - x(k-1)}{\Delta t} \tag{10}$$

where *k* indicates the present sample and *k*-1 the previous sample. By substitution in the previous equations, it is obtained:

$$v_u[k] = -\frac{L_u}{\Delta t}\left(i_{u_{ref}}[k] - i_{u_{ref}}[k-1] - i_{u_{error}}[k]\right) - v_o[k] \tag{11}$$

$$v_l[k] = -\frac{L_l}{\Delta t}\left(i_{l_{ref}}[k] - i_{l_{ref}}[k-1] - i_{l_{error}}[k]\right) + v_o[k] \tag{12}$$

Simplifying the previous equations:

$$v_u[k] = -\frac{L_u}{\Delta t}\left(i_u[k] - i_{u_{ref}}[k-1]\right) - v_o[k] \tag{13}$$

$$v_l[k] = \frac{L_l}{\Delta t}\left(i_{l_{ref}}[k-1] - i_l[k]\right) + v_o[k] \tag{14}$$

Disregarding the circulating currents, according to the current direction arbitrated in the equivalent circuit, the current in each arm are described by the following equations:

$$i_u = -\frac{i_o}{2}, \qquad i_l = \frac{i_o}{2} \tag{15}$$

Substituting in the previous equations, and introducing T_s as the sampling period, the final equations are obtained:

$$v_u[k] = -\frac{L_u}{T_s}\left(\frac{i_{u_{ref}}[k-1]}{2} + i_u[k]\right) - v_o[k] \tag{16}$$

$$v_l[k] = \frac{L_l}{T_s}\left(\frac{i_{l_{ref}}[k-1]}{2} - i_l[k]\right) + v_o[k] \quad (17)$$

The final equations for the reference voltage across each arm, in each sampling period, are used as the modulator signals for the PWM signals generation, adding the necessary offsets for the capacitor balancing in each submodule.

3.3 Capacitor Balancing

Regarding the control of the voltage balancing across the capacitor of the submodules for a single phase MMC with only one arm, as is the case of study, two different steps must be contemplated: the individual voltage control across each submodule, and the arm voltage control [13]. **Fig. 6** presents the individual voltage control of the capacitor in each submodule of the MMC.

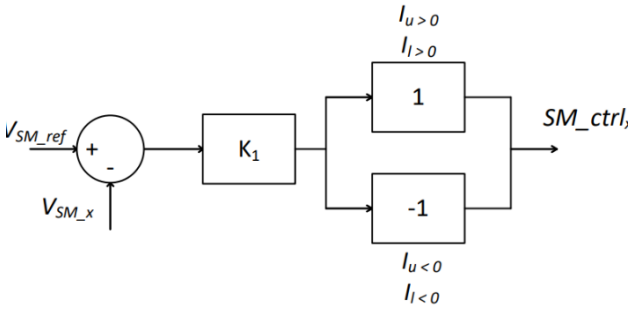

Fig. 6. Individual voltage control of the capacitor in each submodule.

The individual voltage control consists of a proportional control of the voltage of each submodule to follow the voltage reference. Depending on the current direction, the output of the controller is multiplied by 1 if the current in the arm in which the submodule is integrated is positive, or by -1 if the current is the arm is negative. As such, there is a controller unit for every submodule of the MMC. **Fig. 7** presents the voltage control across each arm.

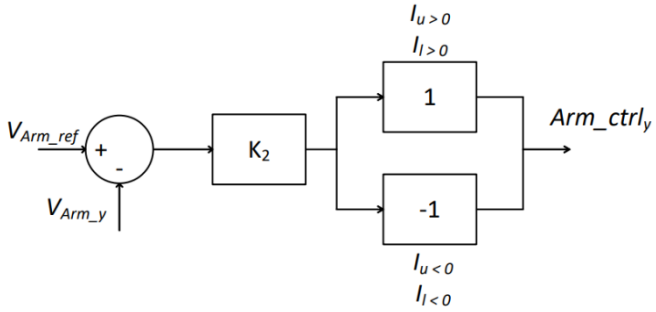

Fig. 7. Voltage control across each arm.

Regarding the arm voltage control, it is similar and works as a complement to the individual voltage control, as it consists of a proportional control of the sum of the submodule voltages across each arm, in order to keep the voltage in each arm balanced. Identical to the individual voltage control, the output of the controller is multiplied by -1 if the current in the arm is negative. Regardless the number of submodules per arm, there are two controller units for arm voltage control.

For the control of the output of the MMC, two different approaches are discussed in this chapter: using a PI controller for the current control, as presented in **Fig. 8**; and using the predictive model control, as presented in **Fig. 9**.

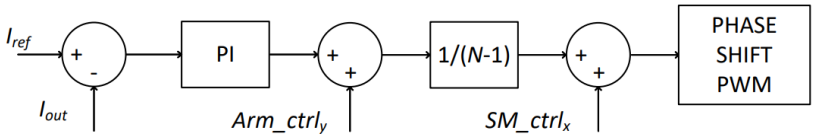

Fig. 8. Gate signal generation for each submodule using a PI controller.

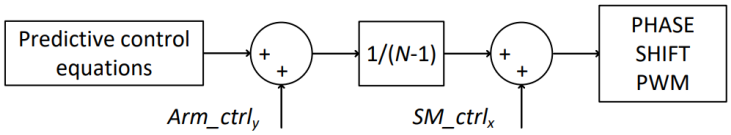

Fig. 9. Gate signal generation for each submodule using model predictive control

Regarding the PI controller, the value of the actual current is subtracted to the reference current value and goes through the proportional and integral gains. Using model predictive control, the final equations are used instead, thus generating the reference signals in both approaches. Then it is summed the output of the arm voltage controllers, followed by a gain of $1/(N-1)$, where N relates to the number of submodules in each arm. Finally, the output of the controller of the voltage of each submodule is summed to the reference signal, having created the modulators for the phase shift PWM.

4 Computational Validation

Regarding power electronics, computer simulation is a powerful tool that allows the validation of both the power and control circuits of the power converters. In this section, computer simulation results are presented for an MMC with 2 submodules in each arm, as follows in **Fig. 10**. The simulation was carried out in the software PSIM, a tool that allows the simulations of both power converter circuits and control schemes for the controllers.

The simulation model presented in **Fig. 10** contains 4 Half-Bridge submodules, 2 in the upper arm and 2 in the lower arm. Each submodule is equipped with a voltage sensor for the monitoring of the voltage across the capacitors in each submodule, in order to keep them balanced to mitigate circulating currents across the power converter, thus reducing power losses and increasing system efficiency. The model is also equipped

with current sensors in both arms for current protection, and a current sensor in the load/grid side to control the converter, using either the PI or the model predictive controller.

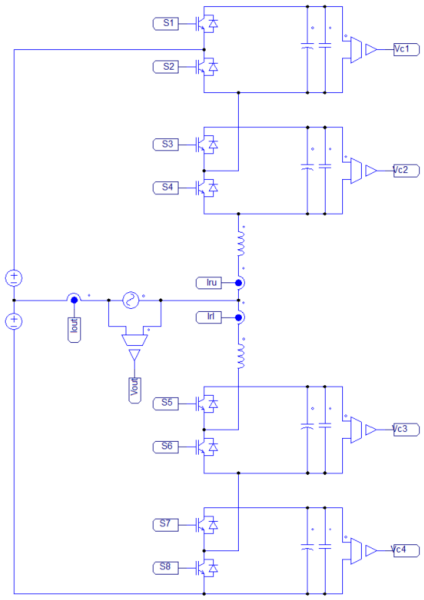

Fig. 10. Schematic of the power circuit of an MMC with 2 submodules in each arm recurring to PSIM simulation software

Table 1: Relevant values used in computer simulation of the MMC

Power Rating	P	1 kW
DC-Link Voltage	v_{dc}	400 V
Inductive filters	L_u, L_l	5 mH
Submodule capacitors	C_{SM}	1.6 mF
Output Voltage (Electrical Power Grid)	v_{out}	230 V
Switching Frequency	f_s	20 kHz

In Table 1, some relevant values for components and ratings, starting with P, the power rating of 1 kW. Each DC-link voltage is 400 V, a necessary value for the interface with the electrical power grid of 230 V, 50 Hz. The power semiconductors switching frequency was arbitrated to 20 kHz. Regarding passive components, the inductive filters used were 5 mH, and the capacitors for the DC-link of each submodule were 1.6 mF.

The modulation technique used was phase-shift carrier PWM since it allows a similar stress level across all the submodules. Regarding the control of the system, results are presented to both techniques, in order to better understand the differences in the results.

Fig. 11 is divided in two parts, both regarding the output of the converter with a PI controller. The first waveform presents the output voltage of the power converter, using line impedance of 5% to better simulate real conditions of power grid interface. The output voltage is 230 V, 50 Hz. The second waveform relates to the output current of the converter for a power rating of 1 kW. The obtained value for the total harmonic distortion of the current waveform is 2%.

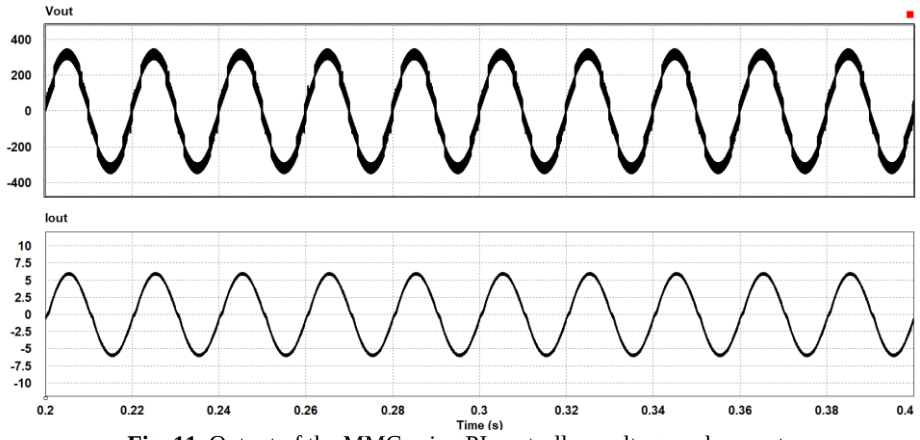

Fig. 11. Output of the MMC using PI controller: voltage and current.

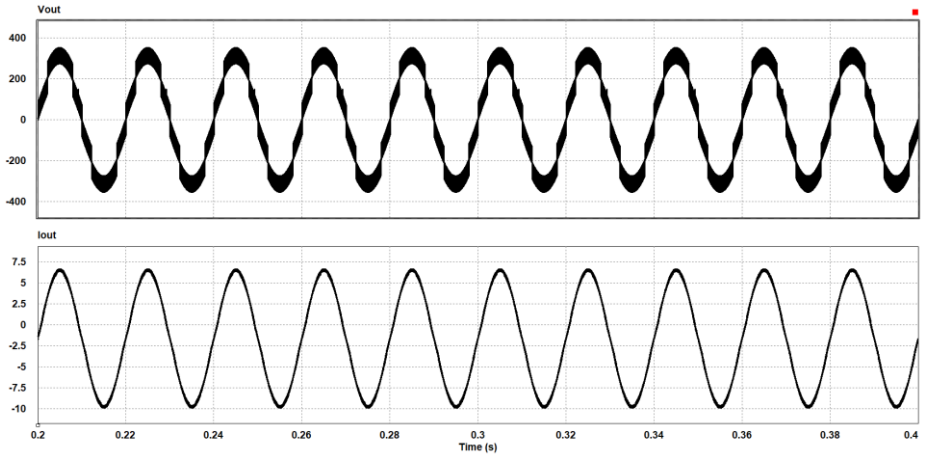

Fig. 12. Output of the MMC using Model Predictive Controller: voltage and current.

In the exact same conditions, changing the control from PI to model predictive, the output of the converter has a similar behavior, as presented in **Fig. 12** possessing however a better quality in the waveform of the current, with a total harmonic distortion of only 0.2%

In **Fig. 13** are presented the voltage waveforms across the 4 submodules that integrate the MMC. The figure is also divided in graphics, each presenting two signals. This first graphic present the waveforms of the upper arm capacitors, and the second graphic

present the lower arm capacitors. As the figure suggests, the voltage across the capacitors of each submodule remains controlled around 400 V, as expected, with approximately 4 V of ripple, corresponding to1% of the steady state value.

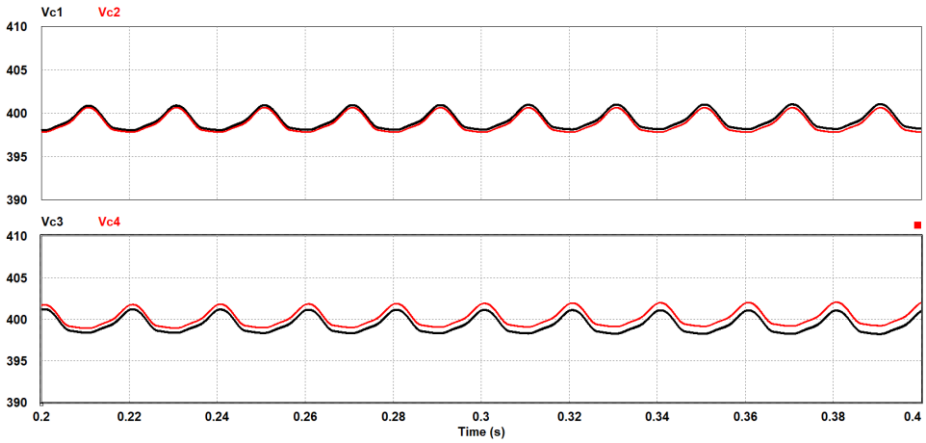

Fig. 13. Submodule voltage across the capacitors of the submodules. Upper arm with V_{c1} and V_{c2}, and lower arm with V_{c3} and V_{c4}.

5 Conclusions

In this paper two different modulation techniques and controllers were discussed, presenting advantages and disadvantages, specifically for MMC applications. Regarding the modulation techniques, the MMC phase-shift carrier allows better results in the functioning of the power converters, due to enabling even power losses across the submodules Regarding control techniques, the PI controller is presented as a simple and intuitive controller, possessing however a larger error in steady-state. The model predictive controller presented suffered some simplifications, such as disregarding the intern resistor of the inductive filters and the circulating currents, due to the complexity of this controller. However complex, this controller possesses a better dynamic response and smaller steady-state error. Recurring to computer simulations, it was possible to verify the behavior of the power converter with both controllers, thus validating the functioning of both the power converter and the control techniques, with differences clearly noticeable in the outcomes. It was also possible to observe that the ripple in the voltage across the capacitor of the submodules is only 1% of the steady state value in both controllers thus mitigating the circulating currents in the MMC and increasing the efficiency of the converter.

Acknowlegments

This work has been supported by FCT – Fundação para a Ciência e Tecnologia within the R&D Units Project Scope: UIDB/00319/2020. This work has been supported by the MEGASOLAR Project POCI-01-0247-FEDER-047220.

References

[1] V. Monteiro, Pinto. J. G., J. C. Ferreira, H. Gonçalves, and J. L. Afonso, 'Bidirectional Multilevel Converter for Electric Vehicles', in *SAAEI 2012 - Annual Seminar on Automation, Industrial Electronics and Instrumentation,* 2012, pp. 434–439.

[2] N. Rodrigues, J. Cunha, V. Monteiro, and J. L. Afonso, 'Technical and Economical Evaluation of Modular Multilevel Converters for the Electrical Power Grid Interface', in *ICEE International Conference on Energy and Environment,* 2022.

[3] J. D. Rogers, 'Comparative Analysis Of Current Control Methods For Modular Multilevel Converters', 2016. [Online]. Available: https://scholarcommons.sc.edu/etd

[4] A. I. Maswood and H. D. Tafti, *Advanced multilevel converters and applications in grid integration*. John Wiley & Sons, 2019.

[5] L. A. M. Barros, M. Tanta, A. P. Martins, J. L. Afonso, and J. G. Pinto, 'Submodule Topologies and PWM Techniques Applied in Modular Multilevel Converters: Review and Analysis', 2020.

[6] A. Yadav, S. N. Singh, and S. P. Das, 'Modular multi-level converter topologies: Present status and key challenges', in *2017 4th IEEE Uttar Pradesh Section International Conference on Electrical, Computer and Electronics (UPCON),* 2017, pp. 280–288. doi: 10.1109/UPCON.2017.8251061.

[7] S. Du, A. Dekka, B. Wu, and N. Zargari, *Modular Multilevel Converters Analysis, Control, and Applications by Sixing Du, Apparao Dekka, Bin Wu, Navid Zargari*. 2018.

[8] F. Martinez-Rodrigo, D. Ramirez, A. B. Rey-Boue, S. de Pablo, and L. C. Herrero-De Lucas, 'Modular multilevel converters: Control and applications', *Energies*, vol. 10, no. 11. MDPI AG, Nov. 01, 2017. doi: 10.3390/en10111709.

[9] E. Solas, G. Abad, J. A. Barrena, S. Aurtenetxea, A. Carcar, and L. Zajac, 'Modular multilevel converter with different submodule concepts-part I: Capacitor voltage balancing method', *IEEE Transactions on Industrial Electronics*, vol. 60, no. 10, pp. 4525–4535, 2013, doi: 10.1109/TIE.2012.2210378.

[10] D. Pathak, G. Sagar, and P. Gaur, 'An Application of Intelligent Non-linear Discrete-PID Controller for MPPT of PV System', in *Procedia Computer Science*, 2020, vol. 167, pp. 1574–1583. doi: 10.1016/j.procs.2020.03.368.

[11] L. Malesani and P. Tenti, 'A novel hysteresis control method for current-controlled voltage-source PWM inverters with constant modulation frequency', *IEEE Trans Ind Appl*, vol. 26, no. 1, pp. 88–92, 1990, doi: 10.1109/28.52678.

[12] S. Orts-Grau, F. J. Gimeno-Sales, A. Abellán-García, S. Seguí-Chilet, and J. C. Alfonso-Gil, 'Improved shunt active power compensator for IEEE standard 1459 compliance', *IEEE Transactions on Power Delivery*, vol. 25, no. 4, pp. 2692–2701, Oct. 2010, doi: 10.1109/TPWRD.2010.2049033.

[13] M. Tanta, J. G. Pinto, V. Monteiro, A. P. Martins, A. S. Carvalho, and J. L. Afonso, 'Deadbeat predictive current control for circulating currents reduction in a modular multilevel converter based rail power conditioner', *Applied Sciences (Switzerland)*, vol. 10, no. 5, Mar. 2020, doi: 10.3390/app10051849.